

An “End-On” Chromium(III)-Superoxo Complex: Crystallographic and Spectroscopic Characterization and Reactivity in C–H Bond Activation of Hydrocarbons

Jaeheung Cho, Jaeyoung Woo, and Wonwoo Nam*

Department of Bioinspired Science, Department of Chemistry and Nano Science, Ewha Womans University, Seoul 120-750, Korea

Received March 2, 2010; E-mail: wwnam@ewha.ac.kr

Oxygen-coordinating metal intermediates, such as metal-superoxo, -peroxo, -hydroperoxo, and -oxo species, play central roles in many biological and catalytic processes.¹ Among the metal–oxygen adducts, metal-superoxo species attracted much attention recently, since the intermediates have been invoked as reactive species in C–H bond activation of substrates in nonheme iron and copper enzymes.^{2,3} In biomimetic and synthetic chemistry, a number of metal-superoxo complexes have been synthesized and characterized with various spectroscopic methods and X-ray crystallography.⁴ However, their reactivity has been rarely explored in C–H bond activation reactions,⁵ although copper(II)-superoxo complexes have recently been shown reactivities in ligand oxidation and the oxidation of organic compounds with weak O–H and N–H bonds.⁶

Mononuclear chromium(III)-superoxo complexes with the superoxo ligand in an end-on (η^1) or side-on (η^2) fashion have been synthesized and characterized spectroscopically.^{7,8} While the molecular structure of a side-on Cr(III)-superoxo complex, [Tp^{iBu,Me}Cr(pz'H)(O₂)]BARF (**A**), was determined by X-ray crystallography,⁸ no crystal structure of end-on Cr(III)-superoxo complexes has been yet reported. Further, while the reactivities of Cr(III)-superoxo species have been reported in hydrogen atom (H-atom) transfer reactions using transition-metal hydrides and hydroperoxides as substrates,^{9,10} the reactivities of chromium-superoxo species have yet to be reported in C–H bond activation reactions. Herein, we report the first crystal structure of an end-on Cr(III)-superoxo complex and the first kinetic studies of C–H bond activation of hydrocarbons by this intermediate.

The starting chromium complex, [Cr^{III}(14-TMC)(Cl)]⁺ (**1**) (14-TMC = 1,4,8,11-tetramethyl-1,4,8,11-tetraazacyclotetradecane), was synthesized and characterized with X-ray crystallography (Figure 1a), UV–vis spectroscopy (Figure 2a), and electrospray ionization mass spectrometry (ESI-MS) (Supporting Information (SI), Figure S1). The crystal structure of **1** shows a vacant site *trans* to the chloride ligand (Figure 1a). Bubbling O₂ through a blue solution of **1** in CH₃CN at –10 °C produced a violet intermediate, **2**, with distinct absorption features at 331 ($\epsilon = 3800 \text{ M}^{-1} \text{ S}^{-1}$), 391 ($\epsilon = 290 \text{ M}^{-1} \text{ S}^{-1}$), 469 ($\epsilon = 150 \text{ M}^{-1} \text{ S}^{-1}$), 549 ($\epsilon = 240 \text{ M}^{-1} \text{ S}^{-1}$), 643 ($\epsilon = 130 \text{ M}^{-1} \text{ S}^{-1}$), and 675 nm ($\epsilon = 140 \text{ M}^{-1} \text{ S}^{-1}$) (Figure 2a). The intermediate persists for several hours at –10 °C. The ESI-MS of **2** exhibits a prominent ion peak at a mass-to-charge (m/z) ratio of 375.0 (Figure 2b), whose mass and isotope distribution pattern correspond to [Cr(14-TMC)(O₂)(Cl)]⁺ (**2**-¹⁶O) (calculated m/z of 375.2). When the reaction was carried out with isotopically labeled ¹⁸O₂, a mass peak corresponding to [Cr(14-TMC)(¹⁸O₂)(Cl)]⁺ (**2**-¹⁸O) appeared at m/z of 379.0 (calculated m/z of 379.2) (Figure 2b, inset). The shift in four mass units on substitution of ¹⁶O with ¹⁸O indicates that **2** contains an O₂ unit.

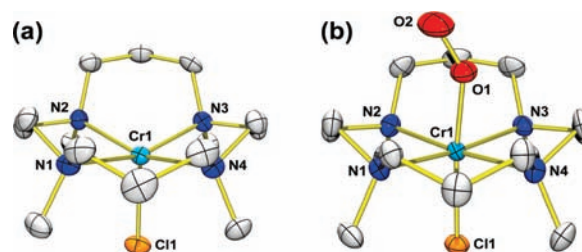


Figure 1. ORTEP plots of (a) [Cr(14-TMC)(Cl)]⁺ (**1**) and (b) [Cr(14-TMC)(O₂)(Cl)]⁺ (**2**) with thermal ellipsoids drawn at the 30% probability level. Hydrogen atoms are omitted for clarity. All four *N*-methyl groups of the 14-TMC ligand in **1** and **2** point toward the chloride ligand. Selected bond lengths (Å) and angles (deg) for **2**: Cr1–O1 1.876(4), Cr1–Cl1 2.3166 (19), O1–O2 1.231(6), Cr1–O1–O2 146.3(4), O1–Cr1–Cl1 174.55(15). See SI Tables S1 and S2 for crystallographic and structural data and Figure S2 for space-filling representations of **1** and **2**.

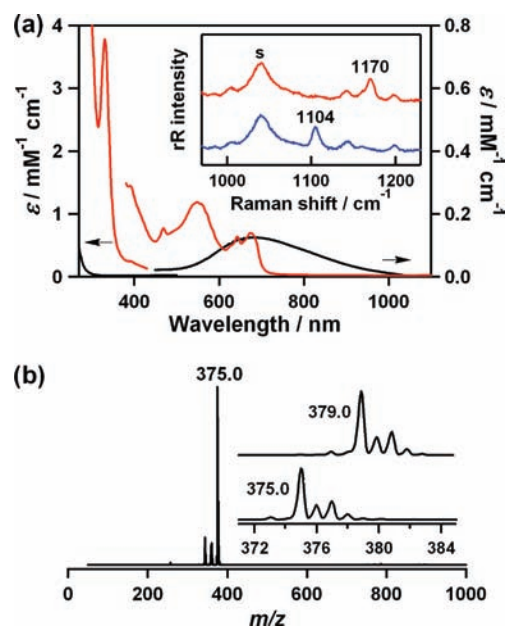


Figure 2. (a) UV–vis absorption spectra of **1** (black line) and **2** (red line) in CH₃CN at –10 °C, where ϵ values from 400 nm should be read in the right-hand axis. Inset shows resonance Raman spectra of **2** prepared with ¹⁶O₂ (red line) and ¹⁸O₂ (blue line). (b) ESI-MS of **2**. Inset shows isotope distribution patterns for **2**-¹⁶O (lower) and **2**-¹⁸O (upper).

The resonance Raman spectrum of **2** (32 mM) was collected using 442-nm excitation in CH₃CN at –20 °C. **2** prepared with ¹⁶O₂ exhibits an isotopically sensitive band at 1170 cm^{-1} , which shifts to 1104 cm^{-1} when ¹⁸O₂ is used, consistent with its assignment as an O–O stretching vibration on the basis of the $^{16}\Delta - ^{18}\Delta$ value

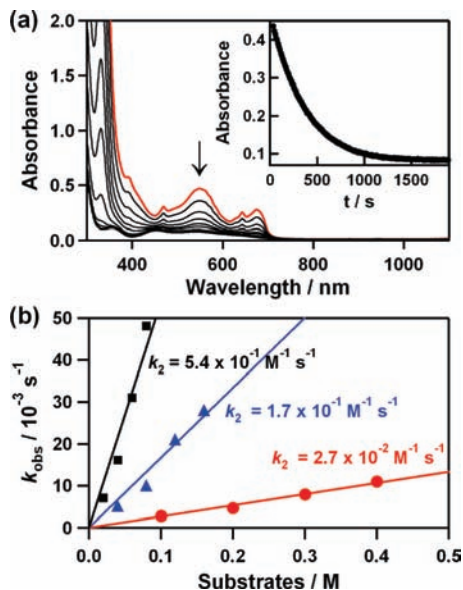


Figure 3. (a) UV-vis spectral changes of **2** (2 mM) upon addition of CHD (50 equiv to **2**, 100 mM) in CH₃CN at -10 °C. Inset shows the time course of the decay of **2** monitored at 550 nm. (b) Plots of k_{obs} against the concentration of xanthene (■), DHA (▲), and CHD (●) to determine second-order rate constants at -10 °C.

of 66 cm^{-1} ($^{16}\Delta - ^{18}\Delta$ (calculated) = 67 cm^{-1}) (Figure 2a, inset).¹¹ This value is comparable to those recorded for spectroscopically characterized end-on Cr(III)-superoxo complexes, such as $[\text{Cr}(\text{O}_2)(\text{H}_2\text{O})_5]^{2+}$ (1166 cm^{-1}) and $[\text{Cr}(\text{cyclam})(\text{O}_2)(\text{H}_2\text{O})]^{2+}$ ($1134/1145$ (doublet) cm^{-1}),⁷ but is higher than that of the side-on Cr(III)-superoxo complex, **A** (1072 cm^{-1}).^{8,11}

The X-ray crystal structure of $2\text{-Cl}\cdot 2\text{CH}_3\text{CN}$ revealed the mononuclear end-on chromium-superoxo complex in a distorted octahedral geometry (Figure 1b). Notably, the O–O bond length ($1.231(6)\text{ \AA}$) of **2** is shorter than that of the side-on Cr(III)-superoxo complex, **A** (1.327 \AA);⁸ the O–O bond length of **2** lies toward the low end of the range of metal-superoxo compounds ($\sim 1.2\text{--}1.3\text{ \AA}$).¹¹ The relatively short O–O bond distance is consistent with the high frequency of the O–O stretching vibration obtained in resonance Raman measurement (vide supra). In addition, the Cr–O bond length (1.876 \AA) of **2** is slightly shorter than the average Cr–O bond length (1.882 \AA) of **A**.⁸ Taken together, the spectroscopic and structural data indicate clearly that **2** is an end-on chromium(III)-superoxo complex.

The oxidative reactivity of **2** was explored in the C–H bond activation of substrates with weak C–H bond dissociation energies (BDEs), such as 1,4-cyclohexadiene (CHD, 78 kcal/mol), 9,10-dihydroanthracene (DHA, 77 kcal/mol), and xanthene (75.5 kcal/mol).¹² Upon reacting **2** with substrates in CH₃CN at -10 °C, the characteristic UV-vis absorption bands of **2** disappeared with a pseudo-first-order decay (Figure 3a), and product analysis of the reaction solutions revealed that benzene ($90 \pm 10\%$), anthracene ($80 \pm 10\%$), and xanthone ($90 \pm 10\%$) were produced in the oxidation of CHD, DHA, and xanthene, respectively. In addition, $[\text{Cr}^{\text{III}}(14\text{-TMC})(\text{OH})(\text{Cl})]^+$ was found in the reaction solutions as a decomposed product of **2** (see SI, Figure S3 for ESI-MS analysis).¹³ The pseudo-first-order rate constants increased proportionally with substrate concentration (Figure 3b), from which second-order rate constants were determined (Figure 3b).¹⁴ We also obtained a kinetic isotope effect (KIE) value of 50(5) in the oxidation of DHA by **2** (see SI, Experimental Section for experimental data). Such a high KIE value implies a hydrogen tunneling mechanism in H-atom abstraction by **2**.¹⁵ Further, this

KIE value is greater than those reported in nonheme iron- and copper-containing enzymes (e.g., KIE values of 8–16),^{2b,c,16,17} where iron(III)- and copper(II)-superoxo species were proposed as reactive species for the C–H cleavage of substrates.^{2,3} The large KIE value, with the dependence of the rate constants on the C–H BDE of substrates, implicates an H-atom abstraction as the rate-determining step for the C–H bond activation by **2**.¹⁸

In conclusion, we have reported the first structurally characterized end-on chromium(III)-superoxo complex, $[\text{Cr}^{\text{III}}(14\text{-TMC})(\text{O}_2)(\text{Cl})]^+$, which was synthesized by reacting $[\text{Cr}^{\text{II}}(14\text{-TMC})(\text{Cl})]^+$ with O₂. The Cr(III)-superoxo intermediate has shown reactivity with activated C–H bonds via a H-atom abstraction mechanism, perhaps supporting the findings that iron- and copper-superoxo intermediates are viable oxidants in nonheme iron- and copper-containing enzymes, respectively.^{2,3}

Acknowledgment. This research was supported by NRF of Korea through CRI and WCU (R31-2008-000-10010-0) Programs. We thank Prof. Takashi Ogura and Dr. Minoru Kubo for assistance in acquiring resonance Raman spectra.

Supporting Information Available: Experimental Section, Tables S1–S2, and Figures S1–S3. This material is available free of charge via the Internet at <http://pubs.acs.org>.

References

- (1) Nam, W. *Acc. Chem. Res.* **2007**, *40*, 465, and review articles in the special issue.
- (2) (a) Bruijninx, P. C. A.; van Koten, G.; Klein Gebbink, R. J. M. *Chem. Soc. Rev.* **2008**, *37*, 2716–2744. (b) Bollinger, J. M., Jr.; Krebs, C. *Curr. Opin. Chem. Biol.* **2007**, *11*, 151–158. (c) Xing, G.; Diao, Y.; Hoffart, L. M.; Barr, E. W.; Prabhu, K. S.; Arner, R. J.; Reddy, C. C.; Krebs, C.; Bollinger, J. M., Jr. *Proc. Natl. Acad. Sci. U.S.A.* **2006**, *103*, 6130–6135.
- (3) (a) Prigge, S. T.; Eipper, B. A.; Mains, R. E.; Amzel, L. M. *Science* **2004**, *304*, 864–867. (b) Chen, P.; Solomon, E. I. *Proc. Natl. Acad. Sci. U.S.A.* **2004**, *101*, 13105–13110. (c) Klinman, J. P. *J. Biol. Chem.* **2006**, *281*, 3013–3016. (d) Rolff, M.; Tuzek, F. *Angew. Chem., Int. Ed.* **2008**, *47*, 2344–2347.
- (4) (a) Klotz, I. M.; Kurtz, D. M., Jr. *Chem. Rev.* **1994**, *94*, 567–568, and review articles in the special issue. (b) Cho, J.; Sarangi, R.; Annaraj, J.; Kim, S. Y.; Kubo, M.; Ogura, T.; Solomon, E. I.; Nam, W. *Nat. Chem.* **2009**, *1*, 568–572. (c) Cramer, C. J.; Tolman, W. B. *Acc. Chem. Res.* **2007**, *40*, 601–608. (d) Itoh, S. *Curr. Opin. Chem. Biol.* **2006**, *10*, 115–122. (e) Yao, S.; Bill, E.; Millsman, C.; Wieghardt, K.; Driess, M. *Angew. Chem., Int. Ed.* **2008**, *47*, 7110–7113. (f) Würtele, C.; Gaoutchenova, E.; Harms, K.; Holthausen, M. C.; Sundermeyer, J.; Schindler, S. *Angew. Chem., Int. Ed.* **2006**, *45*, 3867–3869.
- (5) (a) Kelm, H.; Krüger, H.-J. *Angew. Chem., Int. Ed.* **2001**, *40*, 2344–2348. (b) Abel, E. W.; Pratt, J. M.; Whelan, R.; Wilkinson, P. J. *J. Am. Chem. Soc.* **1974**, *96*, 7119–7120.
- (6) (a) Maiti, D.; Fry, H. C.; Woertink, J. S.; Vance, M. A.; Solomon, E. I.; Karlin, K. D. *J. Am. Chem. Soc.* **2007**, *129*, 264–265. (b) Fujii, T.; Yamaguchi, S.; Hirota, S.; Masuda, H. *Dalton Trans.* **2008**, 164–170. (c) Maiti, D.; Lee, D.-H.; Gaoutchenova, K.; Würtele, C.; Holthausen, M. C.; Narducci Sarjeant, A. A.; Sundermeyer, J.; Schindler, S.; Karlin, K. D. *Angew. Chem., Int. Ed.* **2008**, *47*, 82–85. (d) Kunishita, A.; Kubo, M.; Sugimoto, H.; Ogura, T.; Sato, K.; Takui, T.; Itoh, S. *J. Am. Chem. Soc.* **2009**, *131*, 2788–2789.
- (7) Bakac, A.; Scott, S. L.; Espenson, J. H.; Rodgers, K. R. *J. Am. Chem. Soc.* **1995**, *117*, 6483–6488.
- (8) Qin, K.; Incarvito, C. D.; Rheingold, A. L.; Theopold, K. H. *Angew. Chem., Int. Ed.* **2002**, *41*, 2333–2335.
- (9) Bakac, A. *Coord. Chem. Rev.* **2006**, *250*, 2046–2058.
- (10) (a) Bakac, A. *J. Am. Chem. Soc.* **1997**, *119*, 10726–10731. (b) Vasbinder, M. J.; Bakac, A. *Inorg. Chem.* **2007**, *46*, 2921–2928.
- (11) Cramer, C. J.; Tolman, W. B.; Theopold, K. H.; Rheingold, A. L. *Proc. Natl. Acad. Sci. U.S.A.* **2003**, *100*, 3635–3640.
- (12) (a) Lam, W. W. Y.; Man, W.-L.; Lau, T.-C. *Coord. Chem. Rev.* **2007**, *251*, 2238–2252. (b) Roth, J. P.; Mayer, J. M. *Inorg. Chem.* **1999**, *38*, 2760–2761.
- (13) We propose that $[\text{Cr}^{\text{III}}(14\text{-TMC})(\text{OOH})(\text{Cl})]^+$ is formed upon H-atom abstraction by **2**, followed by the formation of Cr(IV) or V-oxo species via O–O bond cleavage of the Cr(III)–OOH intermediate. The resulting Cr-oxo species might also be involved in the H-atom abstraction reaction, giving the $[\text{Cr}^{\text{III}}(14\text{-TMC})(\text{OH})(\text{Cl})]^+$ product.
- (14) The reactivity of fluorene (BDE of 80 kcal/mol) is ~ 8 times lower than that of CHD. See Experimental Section for data and reaction conditions.
- (15) Costas, M.; Chen, K.; Que, L., Jr. *Coord. Chem. Rev.* **2000**, *200*–202, 517–544.
- (16) Baldwin, J. E.; Abraham, E. *Nat. Prod. Rep.* **1988**, *5*, 129–145.
- (17) Francisco, W. A.; Merkler, D. J.; Blackburn, N. J.; Klinman, J. P. *Biochemistry* **1998**, *37*, 8244–8252.
- (18) (a) Mayer, J. M. *Acc. Chem. Res.* **1998**, *31*, 441–450. (b) Borovik, A. S. *Acc. Chem. Res.* **2005**, *38*, 54–61.

JA1015926